

Examination of the influence of the Saharan Air Layer on hurricanes using data from TRMM, MODIS, and AIRS.

Scott A. Braun¹ and Chung-Lin Shie²

¹ Laboratory for Atmospheres, NASA/Goddard Space Flight Center, Greenbelt, MD

² Goddard Earth Science and Technology Center, University of Maryland, Baltimore County, Baltimore, MD

1. Introduction

The impact of the Saharan air layer (SAL) on the development of tropical cyclones is not well understood. Early studies (e.g., Karyampudi and Carlson 1988) suggested a potential positive influence on the growth of easterly waves and tropical cyclones in the Atlantic. A more recent study by Dunion and Velden (2004, hereafter DV) described several potentially negative influences of the SAL. The reduced Atlantic hurricane activity of 2006 and 2007 compared to 2004 and 2005, particularly as it affected the United States, has led to speculation in the media and in some research papers (Lau and Kim 2007) that dustiness or dry air from increased SAL activity contributed to the decline in hurricane activity in those two years. Map room tropical weather discussions and even planning of field experiments is often focused on the negative impacts of the SAL. But is this intense focus on the negative impacts of the SAL warranted? Is the SAL a major influence, just one of many factors, or is it only a minor influence on Atlantic hurricane activity? These questions led the authors to use National Aeronautics and Space Administration (NASA) satellite data sets to evaluate the role of the SAL in Atlantic hurricane activity.

Synoptic outbreaks of Saharan dust occur from late spring to early fall and can extend

from western Africa across the tropical Atlantic Ocean to the Caribbean (Prospero *et al.* 1970; Prospero and Carlson 1970, 1972). The dust is carried predominantly westward within the SAL, which is caused by strong surface heating as westward moving air crosses the Saharan desert. The heating produces a deep well-mixed layer with warm temperatures and low moisture content. As the warm, dry air moves off the African coast, it is undercut by cooler, moister air to form the elevated SAL. The vertical thermodynamic structure consists of a well-mixed boundary layer capped by the trade wind inversion up to about 850 hPa, where the SAL begins (Carlson and Prospero 1972; Diaz *et al.* 1976; Prospero and Carlson 1981; Karyampudi and Carlson 1988; Karyampudi *et al.* 1999; Karyampudi and Pierce 2002). The SAL extends from ~850 to 500 hPa and is characterized by nearly constant potential temperature and vapor mixing ratio. Temperatures near the top of the SAL tend to be somewhat cooler than the surrounding tropical atmosphere so that the SAL is typically capped by another inversion.

The strong horizontal temperature gradients along the leading and southern borders of the SAL give rise to a maximum in the geostrophic wind (due to thermal wind considerations) to produce the mid-level African Easterly Jet (AEJ) along the southern edge of the SAL. This jet is associated with large vertical and horizontal wind shears and an ageostrophic transverse circulation that produces upward motion in the dust-free air to

Corresponding author: Dr. Scott Braun, NASA/GSFC, Mail Code 613.1, Greenbelt, MD 20771. Scott.A.Braun@nasa.gov.

the south of the jet, leading to deep convection there, and downward motion within the SAL (Karyampudi and Carlson 1988; Karyampudi *et al.* 1999; Karyampudi and Pierce 2002).

Karyampudi and Carlson (1988) and Karyampudi and Pierce (2002) suggested that the SAL contributes to easterly wave growth and, in some cases tropical cyclogenesis, by supporting convection along its leading and southern borders. The SAL increases the strength of the AEJ and its associated vorticity patterns. It leads to weak cyclonic or even anticyclonic potential vorticity (PV) north of the jet, strong positive PV south of the jet, and a significant PV gradient sign reversal. The latter favors easterly wave growth via barotropic instability. Karyampudi and Carlson (1988) also showed that the baroclinic aspects of the AEJ, via the induced ageostrophic circulation and attendant convection, also contribute to wave growth. Thus, Karyampudi and Carlson (1988) and Karyampudi and Pierce (2002) conclude that a strong SAL aids wave growth and tropical cyclone development. However, if dust concentrations are sufficiently high, shortwave radiative heating of the dust layer (Carlson and Benjamin 1980) can lead to reduced ascent south of the jet, thereby suppressing the deep convection needed for wave growth (Randall *et al.* 1984; Karyampudi and Carlson 1988). In other words, the SAL favors tropical cyclogenesis as long as dust concentrations are not too high (with the threshold amount still unknown).

In contrast, DV focused on mechanisms that generally inhibit tropical cyclone genesis and intensification. They suggested that the SAL negatively impacts tropical cyclones in the following ways: 1) The enhanced low-level temperature inversion, maintained by radiative warming of dust, suppresses convective development; 2) vertical wind shear associated with the AEJ inhibits tropical cyclone intensification, based upon studies that have shown that shear tends to weaken storms

(Gray 1968; Merrill 1988; DeMaria and Kaplan 1994, 1999; Frank and Ritchie 2001; Rogers *et al.* 2003; Braun and Wu 2007); and 3) intrusions of dry SAL air into tropical cyclones foster enhanced cold downdrafts (Emanuel 1989; Powell 1990) and lower the convective available potential energy within tropical cyclones. While it was not Dunion and Velden's intention to imply that the SAL's impacts were always negative or were the dominant factor affecting hurricane activity (Dunion and Velden, personal communication), it appears from discussions, media interviews, and research papers (Jones *et al.* 2007; Wu 2007) that some people in the research community have adopted that view.

The results of DV contrast with those of Karyampudi and Carlson (1988) and Karyampudi and Pierce (2002) since the former stress mainly a negative impact of the SAL on tropical cyclones, while the latter suggest a positive influence if dust concentrations are not too high. This disagreement raises questions regarding the role of the SAL in tropical cyclogenesis and intensity change. Our goal with this paper is to assess whether the SAL is a positive or negative influence on tropical cyclogenesis and evolution and to determine if the main negative influences, if present, are the result of vertical shear, warm air (higher stability), or dry air.

2. The SAL: A negative influence?

The work of DV proposed that several mechanisms may be contributing to weakening or preventing the formation of tropical cyclones: (1) vertical shear associated with the AEJ, (2) higher stability associated with the warm layer, and (3) dry air induced cold downdrafts. Here, we examine mechanisms (1) and (2), while (3) will be addressed in the conference presentation.

a. Data

Several NASA satellites currently provide information that is critical to assessing the

impacts of the SAL on hurricanes. The Tropical Rainfall Measuring Mission (TRMM), launched in November 1997, provides information on the rainfall amount and structure in tropical systems over the ocean. Here, we use the TRMM multi-satellite precipitation product (known as the TRMM 3B42 product), which provides rainrate estimates every 3 hours. The Moderate Resolution Imaging Spectroradiometer (MODIS) imager, on both the Aqua and Terra satellites since 2002, provides information on the vertically integrated dust concentration, or aerosol optical depth (AOD), within the SAL. The Atmospheric Infrared Sounder (AIRS) and Advanced Microwave Sounding Unit (AMSU) retrieves temperature and humidity profiles that are essential to characterizing the thermodynamic properties of the SAL. Since the satellite data provide little, if any, wind information, National Centers for Environmental Prediction (NCEP) global analyses, available every 6 h, are used to characterize properties of the AEJ and to complement the satellite data sets. The data are summarized in Table 1. Of particular note regarding the AIRS/AMSU data is that the temperature data for a particular pressure level is the temperature at that level while the relative humidity for a specified level is the layer-averaged RH from the specified level to the next level above. For the discussion that follows, AIRS RH data at 850 hPa (700 hPa) is the average over the layer from 850 to 700 hPa (700 to 600 hPa).

The satellite data are averaged in time to produce daily and monthly analyses. For precipitation, daily analyses show 24-h rainfall accumulation while monthly analyses give the monthly mean rainfall rate. For MODIS AOD and AIRS temperature and relative humidities, daily analyses are created as follows: for grid points with no valid data for a given day, the grid point is assigned a missing value; for one valid data value, the value is taken as the mean value; for multiple valid data values, the

average of the values is used. For MODIS data, monthly mean fields are obtained by averaging the daily results. For AIRS/AMSU, we use the level 3 monthly mean product available from the AIRS data web page.

b. Vertical shear associated with the AEJ

Studies by Frank (1970), Burpee (1972), Landsea and Gray (1992), Thorncroft and Hodges (2001), and Ross and Krishnamurti (2007), among others, have demonstrated that the AEJ plays an instrumental role in the formation of tropical cyclones over the Atlantic, with most storms developing to the south of the AEJ axis. The southern side of the jet is characterized by strong cyclonic vorticity, thereby providing a vorticity-rich environment for cyclogenesis. DV suggested that the AEJ may be a source of vertical wind shear that could negatively impact developing cyclones, but for this to be the case, the cyclones would need to move across the jet or would have to be detrimentally impacted by vertical shear on their periphery. Analysis of NCEP fields for tropical cyclone events between 2003-2007 suggests that developing disturbances generally do not cross the AEJ, but in fact, that the jet provides a key source of vorticity and frequently forms the northern portion of the storm. Hurricanes Florence and Helene in 2006 are provided here as examples (Fig. 1). On 3 September (Fig. 1a), a broad jet is apparent at 700 hPa extending from the western coast of Africa to $\sim 50^\circ\text{W}$ at a latitude of $17\text{-}18^\circ\text{N}$. A region of enhanced cyclonic vorticity (not shown) that would shortly develop into a tropical depression and later into Hurricane Florence is located south of the jet between $40\text{-}50^\circ\text{W}$ and 12°N . By 4 September (not shown), a tropical depression has formed at $\sim 48^\circ\text{W}$, 13°N , with maximum easterlies concentrated on the northern side of the depression in association with the AEJ and strengthening westerlies on the southern side of the storm. The system becomes Tropical Storm Florence on 5 September (Fig. 1c) with

the remnants of the AEJ now comprising the northern part of the storm circulation. Eight days later (Fig. 1e), as Florence moves northeastward off the U.S. east coast, a new wave has emerged off of the western African coast in association with a strong AEJ. As with Florence, a cyclonic vortex develops south of the jet. Over the next 2 days (Fig. 1g), Tropical Storm Helene forms, with the trailing portion of the jet becoming the northern part of the storm circulation. Despite the presence of warm (Figs. 1b, 1d, 1f, 1h) and very dry air (not shown) to the north and west of the storm, Helene intensifies into a Category 1 hurricane by 16 September and a Category 3 hurricane by 18 September.

The relationship between the dust layer, precipitation, the AEJ, and the large-scale meridional circulation is demonstrated in Fig. 2 for 2 September 2006, immediately before the formation of Florence. Strong easterly winds at 700 hPa extend from the African coast to $\sim 50^\circ\text{W}$ with peak winds along or near the southern and leading edges of the dust layer. The heaviest precipitation is located south of the leading portion of the dust outbreak. Meridional cross sections formed by averaging between $20\text{--}40^\circ\text{W}$ show the AEJ centered near $16\text{--}17^\circ\text{N}$ and ~ 650 hPa (Fig. 2b). The vertical circulation exhibits low-level convergence and strong ascent on the south side of the AEJ and sinking motion to the north of the jet. Although there is weak rising motion beneath the jet, deep saturated ascent (Fig. 2c) is confined to the region to the south where vertical shear associated with the AEJ is weak. Thus, the deep convection occurs in the cyclonic vorticity-rich region south of the jet, enabling development of the tropical cyclone. Since the storm does not cross through the jet (Fig. 1), the vertical shear associated with the AEJ does not inhibit development.

The warm SAL air is found to the north of the AEJ (Karyampudi and Carlson 1988), with the developing storms typically located south of the jet very close to the southern edge of the

warm layer (see Fig. 1); in other words, near the zone of strong meridional temperature gradient on the southern side of the SAL. To the extent that the air flow is in geostrophic balance with the thermodynamic field (Cook 1999), the fact that the jet usually forms the northern side of developing storms implies that the warmer air, and hence greater thermodynamic stability, is usually confined to areas north of developing storms. As a result, this higher stability air would not be expected to impact precipitating regions of the storms.

The results in this section are, of course, dependent on the reliability of the NCEP analyses in representing the structure of the AEJ and its relationship to developing tropical cyclones. We have assumed that the relationship between the jet and the storms is correct even if the magnitude of the winds is in error. Comparison of high-resolution aircraft and satellite observations (e.g., from the 2006 NAMMA field campaign) are needed to determine if this assumption is correct.

c. Intensification within the SAL

Assessing the degree to which the SAL is having a negative impact on storm development is difficult without detailed modeling of all the relevant processes and being able to add or remove those processes to determine their impacts. It may be enticing to assume that a storm that struggles to intensify in the presence of SAL air did so because of the SAL, but one risks neglecting other processes that may affect, and perhaps even dominate, intensification. Consider the following four scenarios: 1) No SAL air is present and a storm fails to intensify, 2) no SAL air is present and the storm intensifies, 3) SAL air is present and the storm fails to intensify, and 4) SAL air is present and the storm intensifies. Obviously, in cases (1) and (2), the SAL is not an issue and other processes (vertical shear, other sources of dry air, lack of convective organization, etc.) control whether or not intensification occurs.

If one starts with the hypothesis that the SAL represents a negative influence on tropical cyclone development, then because of cases (1-2), the presence of the SAL near a storm struggling to intensify does not necessarily prove the hypothesis. However, a storm that intensifies in the presence of SAL air would suggest that the SAL may not always, or even often, be a major factor in determining the evolution of a tropical cyclone. Here, we demonstrate a couple of examples of case 4.

The first example is Hurricane Fabian (2003), a portion of whose life cycle is shown in Fig. 3 using TRMM, MODIS, and AIRS observations. On 26 August 2003 (top row), a dust outbreak has recently emerged from the African coast. A convective system at the eastern end of the ITCZ is the seedling for the genesis of Fabian late on 27 August. An AEJ wind maximum (not shown) was located directly on the north side of this convection centered near 21°W, 16°N. The relative humidity pattern in the 850-700 hPa layer shows a narrow zone of maximum RH at the leading edge of the dust with weak precipitation extending northward from the ITCZ within this moist tongue. Air within the dust outbreak possesses lower humidities (~20-40%). Very warm air at 850 hPa extends from Africa to nearly 40°W to the north of the ITCZ and the seedling disturbance. Two days later (second row), the dust has pushed westward, with the greatest concentration just north and ahead of Fabian, now a tropical depression. The moist tongue is still at the leading edge of the dust outbreak, with more enhanced precipitation occurring at the northern end of the moist tongue. Dry air (30-40% relative humidity) surrounds the tropical depression from east to north and west. Fabian is situated on the southern edge of the warm SAL air, about 10° longitude behind the leading edge of the SAL. By 30 August (third row), dust concentrations have diminished with AOD values of ~0.3-0.4 surrounding Fabian, which at this time has intensified into

a category 2 hurricane. Relative humidities in the northern half of the storm's environment range from between 40-60%. Fabian remains along the southern edge of the warm air, which is gradually cooling and shrinking with time. Finally, by 1 September (bottom row), Fabian has intensified into a category 4 hurricane. It continues to be surrounded by low to moderate concentrations of dust (again, AOD between 0.3-0.4). Relative humidities are as low as 30% to the east of the storm, 40-60% to the west, and Fabian is now to the east of what is left of the warm air. Fabian peaks in intensity at the beginning of 2 September and maintains category 4 strength through much of 3 September. By that time (not shown), a new dust outbreak is just beginning at the African coast, where soon another convective disturbance will emerge and evolve under similar circumstances to become Hurricane Isabel with category 5 intensity.

The year 2006 saw diminished hurricane activity in the Atlantic region, which has been attributed by some (Lau and Kim 2007) to be partly the result of enhanced dust activity that year, while others have argued for other causes such as El Nino (Bell et al. 2007). Field experiments such as the NASA African Monsoon Multidisciplinary Analyses (NAMMA) experiment over the eastern Atlantic Ocean focused considerable attention on dust, the SAL, and the low tropical cyclone activity that year. Hurricane Helene was one of the strongest hurricanes in 2006. Its development was similar to Fabian's in that the storm intensified to category 3 intensity despite the presence of SAL air. On 13 September 2006, Helene was a tropical depression that formed south of a significant dust outbreak. By this time, the dusty air was moving rapidly ahead of the storm, with the highest dust concentrations northwest of the storm. Very warm and dry air (20-40% RH) was present to the north of the storm associated with strong easterly flow in the AEJ. By 16 September, much of the dust had

raced ahead of Helene (although AODs of $\sim 0.2-0.3$ still surrounded Helene). Very dry air with RH $\sim 20\%$ surrounded Helene to the north, with values between 30-60% swirling around into the southern side of the storm. Despite this very dry air, Helene became a hurricane later that day and intensified into a category 3 storm by 18 September. While Helene was able to intensify into a category 3 storm, it is possible that the dry air slowed the rate of intensification or helped to limit intensity to category 3 instead of 4 or 5.

The storms highlighted by DV present examples in which dry SAL air may have limited or suppressed hurricane development, although other potential causes for storm intensity change were not examined. The examples described above, however, emphasize that the presence of dry SAL air surrounding a tropical disturbance does not necessarily imply that the storm will struggle to intensify. Based upon examination of AIRS-derived 850-600 hPa RH data for 2003-2007, we find that dry air in the immediate vicinity of developing tropical cyclones is a rather common occurrence. The puzzle, then, for atmospheric scientists to solve is determining what factors make some storms more susceptible to dry air and others rather immune to it? Is it related more to characteristics of the environment such as vertical wind shear, to characteristics of the vortex (size, strength), or to other factors such as the marsupial hypothesis of Dunkerton et al. (2008)?

3. Conclusions

Previous studies on the impact of the Saharan Air Layer on tropical cyclone genesis and intensification have yielded mixed results, with some studies (Karyampudi and Carlson 1988; Karyampudi et al. 1999; Karyampudi and Pierce 2002) suggesting that the SAL can have a positive influence on development when dust concentrations are not too high, while other studies (Dunion and Velden 2004; Jones et al. 2007) have suggested that the SAL

is primarily a negative influence. Dunion and Velden (2004) describe several ways by which the SAL can inhibit tropical cyclone growth including low-level vertical wind shear associated with the African Easterly Jet, increased thermodynamic stability caused by the elevated warm layer, and impacts of dry mid-level air, particularly in terms of the production of cold downdrafts. In this study, we use NASA satellite remote sensing data and NCEP global analyses to evaluate the negative impacts proposed by DV.

The AEJ generally does not produce vertical wind shear over developing disturbances. Instead, convective systems typically form on the southern side of the AEJ, where the background cyclonic vorticity is high and the large-scale meridional circulation favors upward motion. At very early stages of development, the AEJ may stretch from Africa to some distance over the Atlantic. As storm systems develop south of the jet, an easterly wind maximum is seen to break off from the jet to form the northern part of the developing cyclonic storm. Since the disturbances do not cross the jet, but in fact the jet forms the northern side of the storm systems, no vertical shear is felt over the center of the storms. Hence, there appears to be little negative influence caused by vertical wind shear associated with the AEJ.

The warm SAL air is found to the north of the AEJ, with the developing storms typically located south of the jet very close to the southern edge of the warm layer, in other words, near the zone of strong meridional temperature gradient on the southern side of the SAL. To the extent that the air flow is in geostrophic balance with the thermodynamic field, the fact that the jet usually forms the northern side of the storms implies that the warmer air, and hence greater thermodynamic stability, is usually confined to areas north of developing storms. As a result, this higher stability air generally does not impact precipitating regions of the storms.

The presence of dry air in the environment of storms is also not a good indicator of whether or not a storm will intensify. While some storms appear to be weakened by the presence of dry SAL air, cases can be found in which storms readily intensify despite the presence of dry air in their immediate surroundings. The question to be addressed in future research is why some storms are able to intensify while others are not. Research on this topic is ongoing.

4. References

- Aumann, H.H., M.T. Chahine, C. Gautier, M.D. Goldberg, E. Kalnay, L.M. McMillin, H. Revercomb, P.W. Rosenkranz, W.L. Smith, D.H. Staelin, L.L. Strow, and J. Susskind: "AIRS/AMSU/HSB on the Aqua mission: design, science objectives, data products, and processing systems," *IEEE Trans. Geosci. Remote Sensing*, **41**, 253-264, 2003.
- Bell, G., E. Blake, C. Landsea, M. Chelliah, R. Pasch, K. Mo, and S. Goldenberg, 2007: The 2006 North Atlantic hurricane season: A climate perspective. *Bull. Amer. Meteor. Soc.*, (submitted).
- Braun, S. A. and L. Wu 2007: A numerical study of Hurricane Erin (2001). Part II: Shear and the organization of eyewall vertical motion. *Mon. Wea. Rev.*, **135**, 1179-1194.
- Burpee, R. W., 1972: The origin and structure of easterly waves in the lower troposphere of North Africa. *J. Atmos. Sci.*, **29**, 77-90.
- Carlson, T.N., and J.M. Prospero, 1972: The large-scale movement of Saharan air outbreaks over the northern equatorial Atlantic. *J. Appl. Meteor.*, **11**, 283-297.
- , and S.G. Benjamin, 1980: Radiative heating rates of Saharan dust. *J. Atmos. Sci.*, **37**, 193-213.
- Cook, K. H., 1999: Generation of the African easterly jet and its role in determining West African Precipitation. *J. Climate*, **12**, 1165-1184.
- Diaz, H.F., T.N. Carlson, and J.M. Prospero, 1976: A study of the structure and dynamics of the Saharan air layer over the northern equatorial Atlantic during BOMEX. National Hurricane and Experimental Meteorology Laboratory NOAA Tech. Memo. ERL WMPO-32, 61 pp.
- DeMaria, M., and J. Kaplan, 1994: A Statistical Hurricane Intensity Prediction Scheme (SHIPS) for the Atlantic basin. *Wea. Forecasting*, **9**, 209-220.
- , and ———, 1999: An updated statistical hurricane intensity prediction scheme (SHIPS) for the Atlantic and eastern North Pacific Basins. *Wea. Forecasting*, **14**, 326-337.
- Dunion, J.P. and C.S. Velden, 2004: The impact of the Saharan air layer on Atlantic tropical cyclone activity, *Bull. Amer. Meteor. Soc.*, 353-365.
- Dunkerton, T. J., M. T. Montgomery, and Z. Wang, 2008: Tropical cyclogenesis in a tropical wave critical layer: Easterly waves. *Atmos. Chem. Phys.*, (submitted).
- Emanuel, K.A., 1989: The finite-amplitude nature of tropical cyclogenesis. *J. Atmos. Sci.*, **46**, 3431-3456.
- Frank, N. L., 1970: Atlantic tropical systems of 1969. *Mon. Wea. Rev.*, **98**, 307-314.
- Frank, W.M., and E.A. Ritchie, 2001: Effects of vertical wind shear on the intensity and structure of numerically simulated hurricanes. *Mon. Wea. Rev.*, **129**, 2249-2269.
- Gray, W.M., 1968: Global view of the origin of tropical disturbances and storms. *Mon. Wea. Rev.*, **96**, 669-700.
- Huffman, G.J., R.F. Adler, D.T. Bolvin, G. Gu, E.J. Nelkin, K.P. Bowman, E.F. Stocker, D.B. Wolff, 2007: The TRMM Multi-satellite Precipitation Analysis: Quasi-Global, Multi-Year, Combined-

- Sensor Precipitation Estimates at Fine Scale. *J. Hydrometeor.*, **8**, 38-55.
- Jones, T. A., D. J. Cecil, and J. Dunion, 2007: The environmental and inner-core conditions governing the intensity of Hurricane Erin (2007). *Wea. Forecasting*, **22**, 708-725.
- Karyampudi, V.M., and T.N. Carlson, 1988: Analysis and numerical simulations of the Saharan air layer and its effect on easterly wave disturbances. *J. Atmos. Sci.*, **45**, 3102-3136.
- , and H.F. Pierce, 2002: Synoptic-scale influence of the Saharan air layer on tropical cyclogenesis over the Eastern Atlantic. *Mon. Wea. Rev.*, **130**, 3100-3128.
- , and Coauthors, 1999: Validation of the Saharan dust plume conceptual model using lidar, Meteosat, and ECMWF data. *Bull. Amer. Meteor. Soc.*, **80**, 1045-1075.
- Landsea, C. W., and W. M. Gray, 1992: The strong association between Western Sahelian monsoon rainfall and intense Atlantic hurricanes. *J. Climate*, **5**, 435-453.
- Lau, K. M., and J. M. Kim, 2007: How nature foiled the 2006 hurricane forecasts. *EOS Trans.*, **88**, No. 9, 105-107.
- Merrill, R.T., 1988: Environmental influences on hurricane intensification. *J. Atmos. Sci.*, **45**, 1678-1687.
- Powell, M.D., 1990: Boundary layer structure and dynamics in outer hurricane rainbands. Part II: Downdraft modification and mixed-layer recovery. *Mon. Wea. Rev.*, **118**, 918-938.
- Prospero, J.M., and T.N. Carlson, 1970: Radon-222 in the north Atlantic trade winds: Its relationship to dust transport from Africa. *Science*, **167**, 974-977.
- , and ———, 1972: Vertical areal distributions of Saharan dust over the western equatorial North Atlantic Ocean. *J. Geophys. Res.*, **77**, 5255-5265.
- , and ———, 1981: Saharan dust outbreaks over the tropical North Atlantic. *Pure Appl. Geophys.*, **119**, 677-691.
- , E. Bonatti, C. Schubert, and T.N. Carlson, 1970: Dust in the Caribbean atmosphere traced to an African dust storm. *Earth Planetary Science Letters*, **9**, 287-293.
- Randall, D., T.N. Carlson, and Y. Mintz, 1984: The sensitivity of a general circulation model to Saharan dust heating. *Aerosols and Their Climate Effects*, H. E. Gerber and A. Deepak, Eds., Deepak Publishing, 123-132.
- Rogers, R, S. Chen, J. Tenerelli, and H. Willoughby, 2003: A numerical study of the impact of vertical shear on the distribution of rainfall in Hurricane Bonnie (1998), *Mon. Wea. Rev.*, **131**, 1577-1599.
- Ross, R. S., and T. N. Krishnamurti, 2007: Low-level African easterly wave activity and its relation to Atlantic tropical cyclogenesis in 2001. *Mon. Wea. Rev.*, **135**, 3950-3964.
- Salomonson V.V., W.L. Barnes, P.W. Maymon, H.E. Montgomery and H. Ostrow, 1989: MODIS: Advanced Facility Instrument for Studies of the Earth as a System, *IEEE Trans. on Geos. and Rem. Sens.*, **27**, 145-153.
- Thorncroft, C. D., and K. Hodges, 2001: African easterly wave variability and its relationship to Atlantic tropical cyclone activity. *J. Climate*, **14**, 1166-1179.
- Wu, L., 2007: Impact of Saharan air layer on hurricane peak intensity. *Geophys. Res. Lett.*, **34**, doi:10.1029/2007GL029564.

Table 1. Summary of the data used in this study.

Data Set	Measurement	Horizontal Resolution	Frequency	Description
TRMM	Rainfall rate (mm h ⁻¹)	0.25°	3 h	TRMM multi-satellite precipitation product (3B42) (Huffman et al. 2007)
MODIS	AOD	1°	24 h	MODIS Level 3 product (Salomonson et al. 1989)
AIRS	Temperature, relative humidity profiles	1°	12 h	AIRS Level 3 product, 13 vertical levels in troposphere (Aumann et al. 2003)
NCEP	3D winds, temperature, relative humidity	1°	6 h	NCEP final analyses archived at NCAR

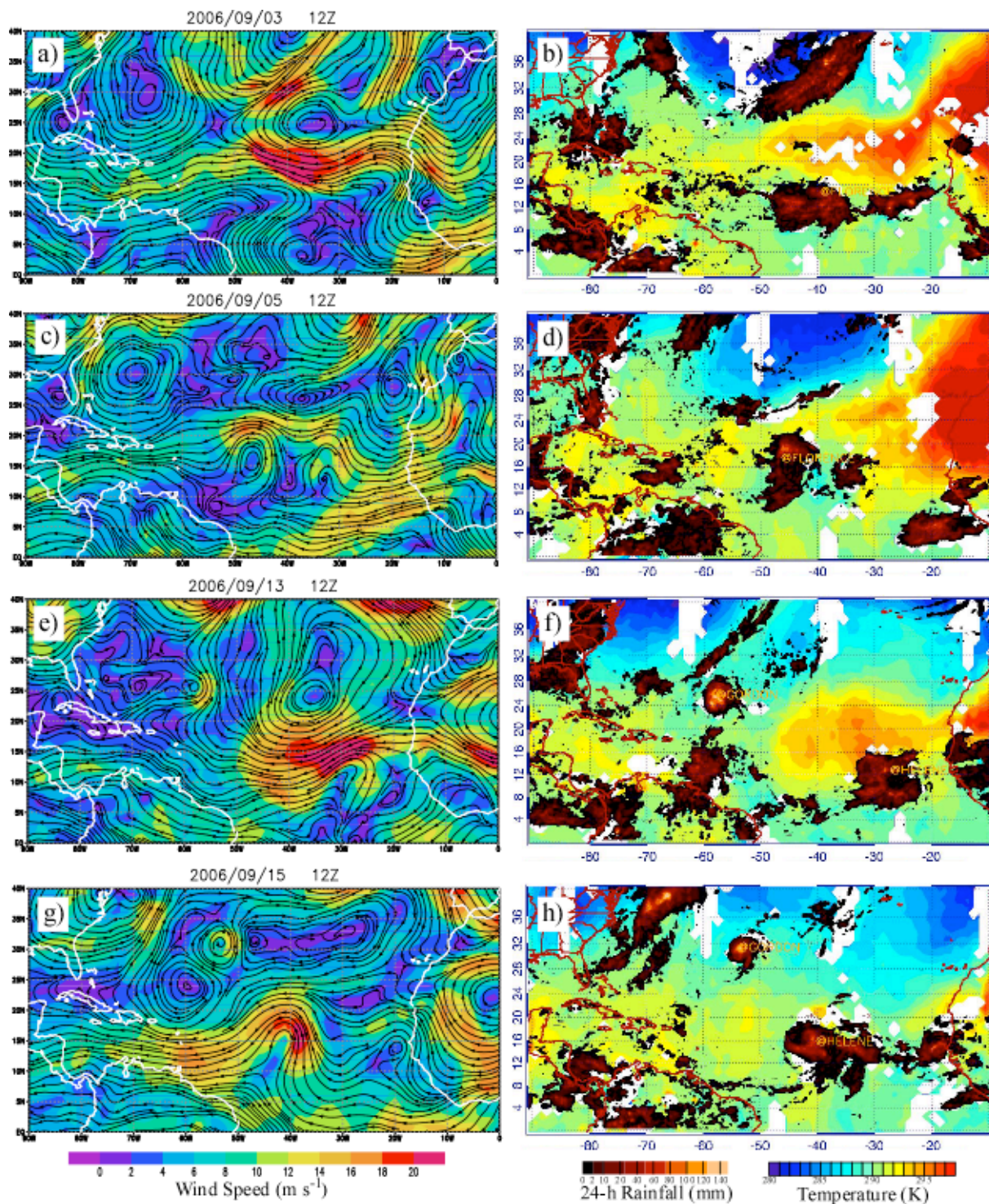


Figure 1. (Left column) NCEP analyzed isotachs and streamlines at 700-hPa for the indicated days and times. Plots show the evolution of the easterly jet for hurricanes Florence and Helene in September 2006. (Right column) The corresponding AIRS 850-hPa temperature and TRMM 24-h accumulated rainfall analyses.

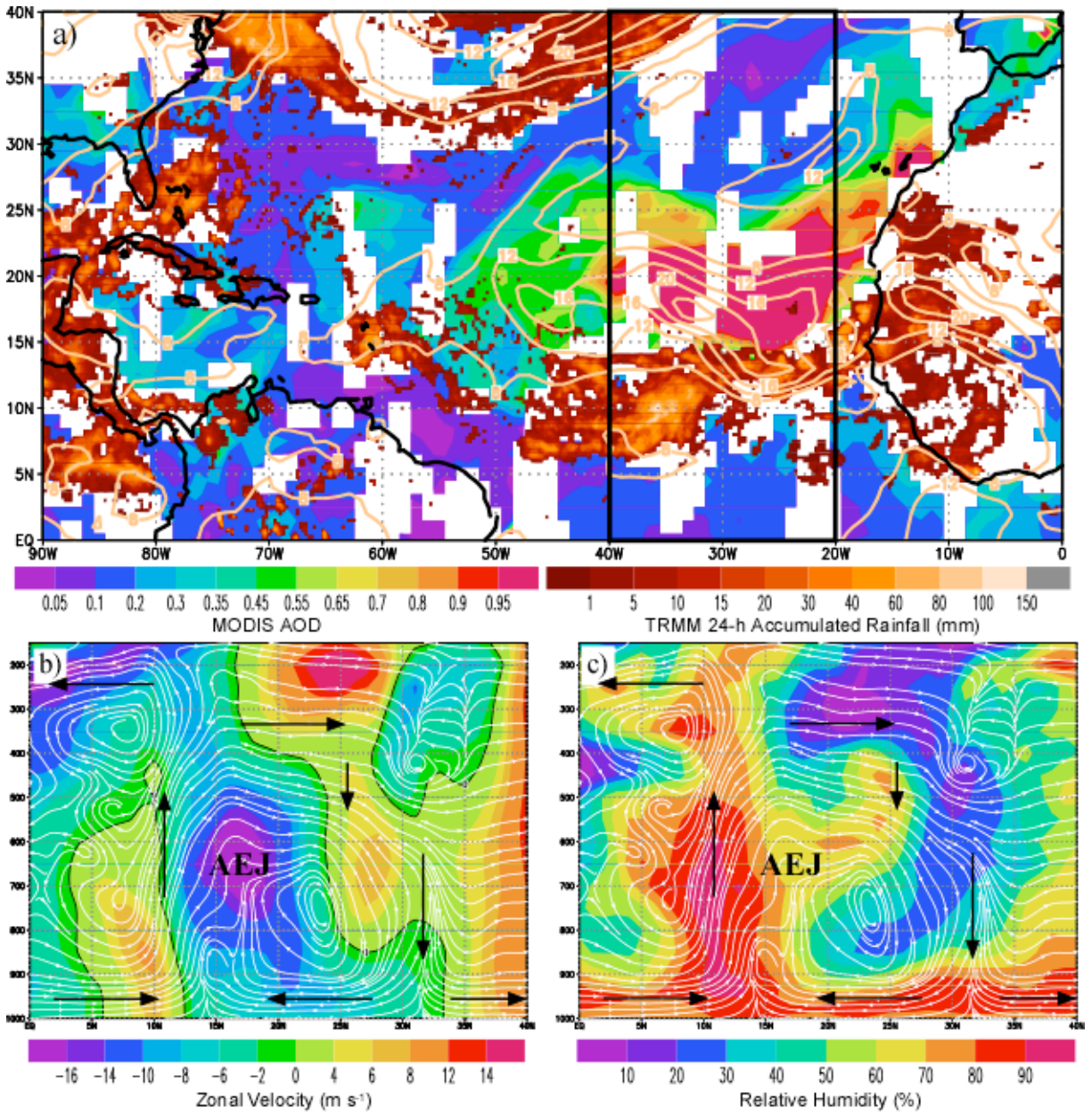


Figure 2. (a) MODIS AOD, TRMM 24-h accumulated rainfall, and NCEP 700-hPa winds (isotachs, contours at 4 m s^{-1} intervals starting at 8 m s^{-1}) for 12 UTC 2 September 2006. (b-c) Vertical cross sections of meridional circulation (streamlines) and (b) zonal wind and (c) RH averaged between $20\text{-}40^\circ\text{W}$ longitude. The location of the AEJ is indicated while arrows highlight the direction of the mean circulation.

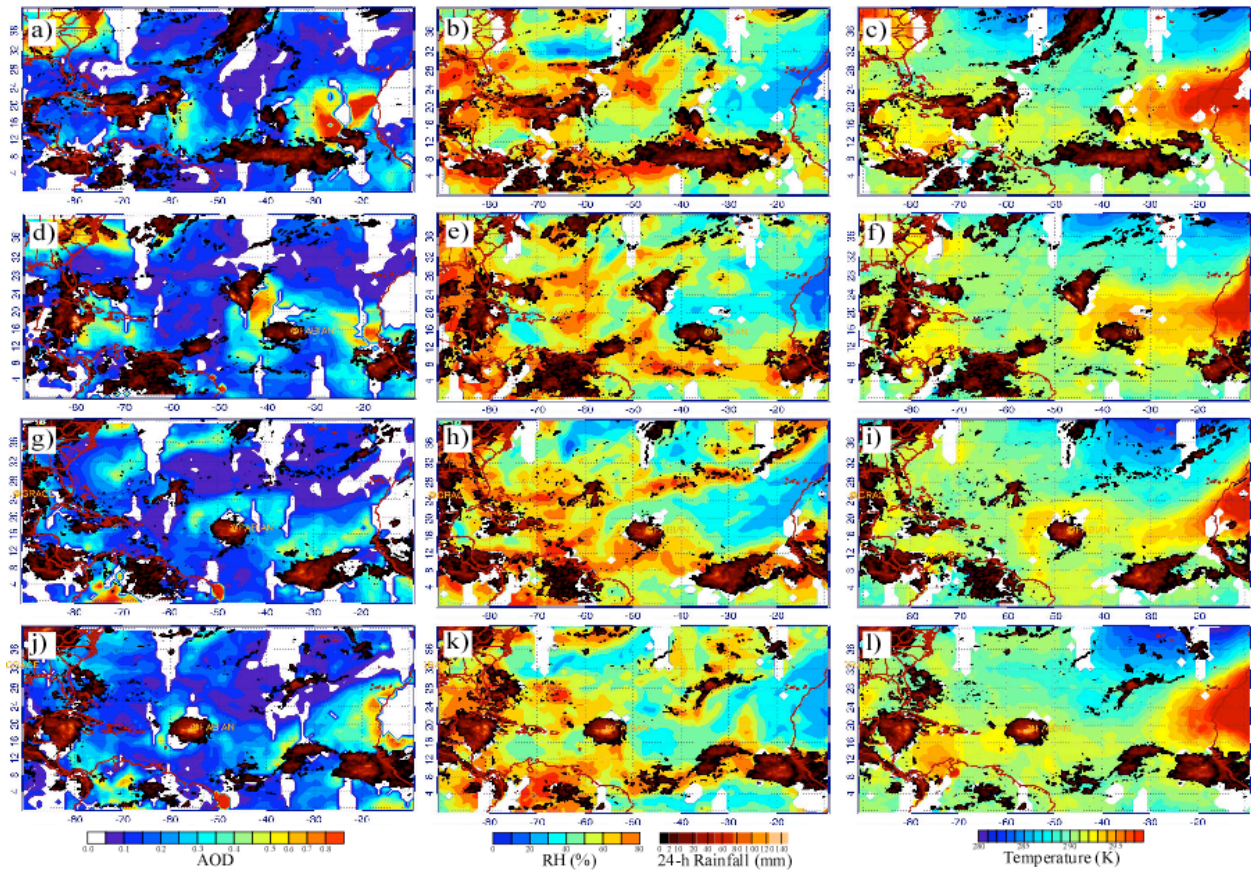


Figure 3. TRMM 24-h accumulated rainfall (orange color shading) and (left) MODIS AOD, (middle) AIRS 850-700-hPa RH, and (right) AIRS 850-hPa temperature for (top row) 26 August 2003, (second row) 28 August, (third row) 30 August, and (bottom row) 1 September.